Supporting Information

Probing Fluorescence Resonance Energy Transfer and Hole Transfer in Organic Solar Cells Using a Tandem Structure

Zhenmin Zhao,[a] Shenglong Chu,[b] Jie Lv,[c] Qianqian Chen,[c] Zhengguo Xiao,[b] Shirong Lu,[d] Zhipeng Kan[a,e]*

[a] *Center on Nano Energy Research, Guangxi Colleges and Universities Key Laboratory of Blue Energy and Systems Integration, carbon peak and neutrality science and technology development institute, School of Physical Science & Technology, Guangxi University, Nanning 530004, China.*
[b] *Hefei National Laboratory for Physical Science at the Microscale, Department of Physics, CAS Key Laboratory of Strongly-Coupled Quantum Matter Physics, University of Science and Technology of China, Hefei, Anhui 230026, China.*
[c] *Thin-film Solar Technology Research Center, Chongqing Institute of Green and Intelligent Technology, Chinese Academy of Sciences, Chongqing 400714, P. R. China.*
[d] *Department of Material Science and Technology, Taizhou University, Taizhou 318000, China.*
[e] *State Key Laboratory of Featured Metal Materials and Life-cycle Safety for Composite Structures, Nanning 530004, China.*

*Corresponding author.
* *Zhipeng Kan. E-mail: kanzhipeng@gxu.edu.cn*

1. Experimental Section/Methods.....3

2. Energy level of PTO2, IDTT-IC and IDTT-4FIC.....5

3. Calculation of Förster radius R_0.....6

4. Temperature-dependent PL spectra 8

5. Devices structure 9

6. Performance of devices with PEDOT:PSS intercalation 10

7. Photovoltaic performance of the BHJ OSCs 13

8. References 14

1. Experimental Section/Methods

Materials. PTO2 was purchased from Solarmer Co., Ltd. (Beijing, China). PEDOT:PSS and PDIN were purchased from Energy Chemical., Ltd. These materials were used as received without further treatment. IDTT-IC and IDTT-4FIC were synthesized according to the method reported.

Device Fabrication. BHJ organic solar cells were prepared on glass substrates with tin doped indium oxide (ITO, 15 Ω/sq) (device area: 0.1 cm^2). Substrates were prewashed with isopropanol to remove organic residues before immersing in an ultrasonic bath of soap for 15 min. Samples were rinsed in flowing deionized water for 5 min before being sonicated for 15 min each in successive baths of deionized water, acetone and isopropanol. Next, the samples were dried with pressurized nitrogen before being exposed to a UV-ozone plasma for 15 min. A thin layer of PEDOT:PSS (~20 nm) (Clevios AL4083) was spin-coated onto the UV-treated substrates, the PEDOT-coated substrates were subsequently annealed on a hot plate at 160 °C for 15 min, and the substrates were then transferred into the glovebox for active layer deposition.

All solutions were prepared in the nitrogen filled glove box. Optimized devices were both obtained by dissolving PTO2/IDTT-4FIC or PTO2/IDTT-IC in chlorobenzene (CB) using a D/A ratio of 1:1 (wt/wt), total concentration of 24 mg/ml. The as-prepared solutions were stirred 3 hours at 60 °C before being cast on the PEDOT:PSS substrates. The active layers were spin-coated at an optimized speed of 1500 rpm. For devices based on PTO2/PEDOT:PSS/IDTT-IC(IDTT-4FIC), the PTO2 (CB, 8mg/mL) was spin-coated with a speed of 1500 rpm. Then PEDOT: PSS with isopropanol as solvent was spin coated on PTO2, and different film thicknesses of PEDOT: PSS are obtained by controlling the spin speed. Finally, IDTT-IC or IDTT-4FIC (DCM, 8mg/mL) was spin coated with a speed of 3000 rpm.

Next, a ~10nm-thin layer of PDIN was coated on top as electron transport layer. And then the substrates were pumped down in high vacuum at a pressure of 3×10^{-4} Pa, and Ag layer (100 nm) was thermally evaporated onto the active layer.

Photocurrent measurements. The J−V measurement was performed via a XES-50S1 (SAN-EI Electric Co., Ltd.) solar simulator (AAA grade) whose intensity was calibrated by a certified standard silicon solar cell (SRC-2020, Enlitech) under illumination of AM 1.5G 100 mW cm−2. The AM 1.5G light source with a spectral mismatch factor of 1.01 was calibrated by the National Institute of Metrology. The intensity of the AM 1.5G spectra was calibrated by a certified standard silicon solar cell (SRC-2020, Enlitech) calibrated by the National Institute of Metrology. The J-V curves of small-area devices were measured in forwarding scan mode (from -0.2 V to 1.2 V) with a scan step length of 0.02 V. The external quantum efficiency (EQE) was measured by a certified incident photon to electron conversion (IPCE) equipment (QE-R) from Enli Technology Co., Lt. The light intensity at each wavelength was calibrated using a standard monocrystalline Si photovoltaic cell.

Photoelectron spectroscopy in air (PESA) measurements. Photoelectron spectroscopy in air (PESA) measurements were recorded using a Riken Keiki PESA spectrometer with a power setting of 10 nW and a power number of 0.3. Samples for PESA were prepared on glass substrates.

Temperature-dependent PL measurements. The emission spectra were recorded with a Horiba Fluorolog-3 system. The Temperature-dependent PL spectra of each blend in the temperature range of 100 to 280 K were recorded under 500 nm light excitation. The film was initially cooled to 100K and the PL spectrum was recorded when it was heated to 280K at 20K temperature interval.

Photoluminescence quantum yield measurements. The photoluminescence quantum yield (ϕ) of the PTO2 was measured by a OmniFluo990LSP equipped with an integrating hemisphere at an excitation wavelength of 500 nm.

2. Energy level of PTO2, IDTT-IC and IDTT-4FIC

The IE was measured by photoelectron spectroscopy in air as shown in Fig. S1a. The EA was estimated by adding the optical bandgap. The optical bandgap was determined by the intersection of normalized absorbance spectra and normalized PL spectra [1].

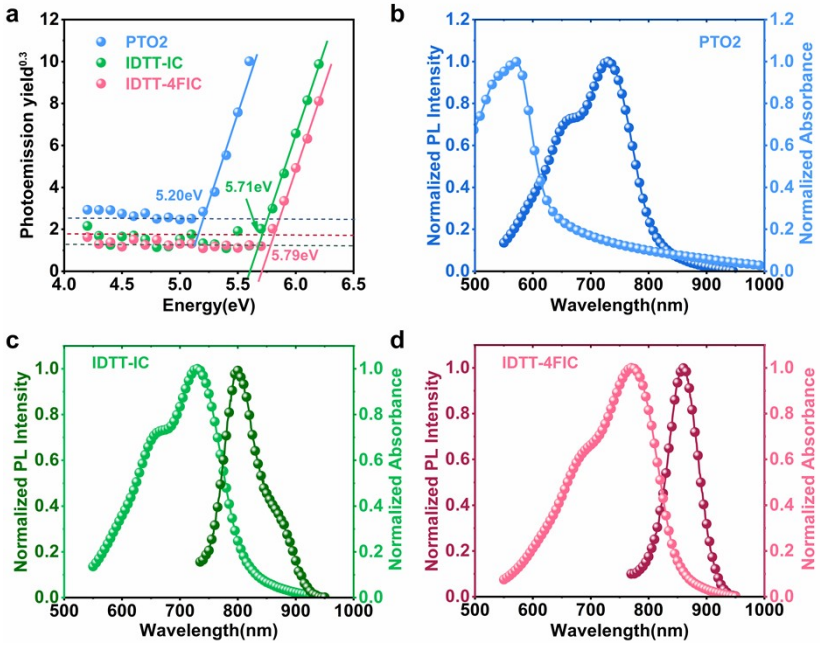

Fig. S1 | The energy level of PTO2, IDTT-IC and IDTT-4FIC. a, PESA results of neat films of PTO2, IDTT-IC and IDTT-4FIC. Normalized PL and absorption spectra of **b,** PTO2, **c,** IDTT-IC and d, IDTT-4FIC.

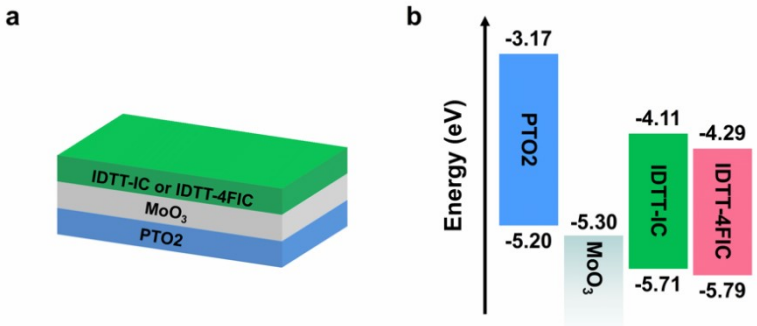

Fig. S2 | Schematic diagram and energy level of PTO2/MoO_3/IDTT-IC (or IDTT-4FIC). a, Schematic diagram of the tandem film structure. **b,** energy level of each layer used in this work.

3. Calculation of Förster radius R_0

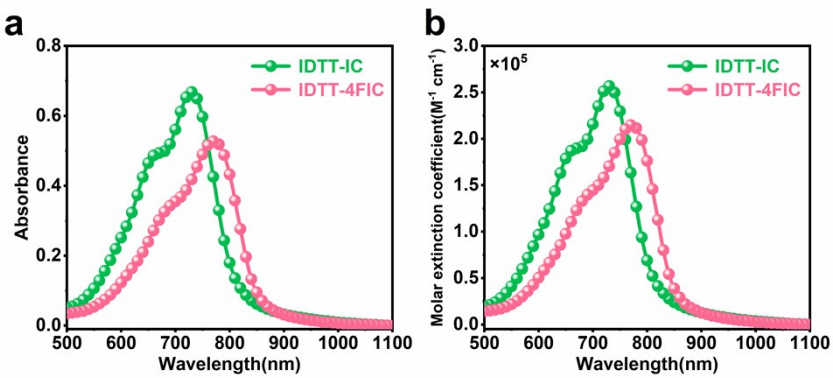

Fig. S3 | Absorbance spectra (a) and molar extinction coefficient spectra (b) of IDTT-IC and IDTT-4FIC.

The Förster radius (R_0) was calculated by the PL spectrum in PTO2 films and the absorption spectrum in IDTT-IC (or IDTT-4FIC) films, and can be calculated by:

$$R_0 = 0.0211\left(\frac{\kappa^2 \Theta_D J(\lambda)}{n^4}\right)^{\frac{1}{6}} \quad (1)$$

where, Θ_D is the quantum efficiency of the donor, n is the refractive index. The value of n is 1.4, and the absolute quantum efficiency of PTO2 is equal to 8.5%. κ^2 depends on the relative orientation of donor and acceptor dipoles, this value varies from 0 to 4, for randomly oriented dipoles κ^2=2/3.

The $J(\lambda)$ is the overlap region between the acceptor absorption spectrum and the normalized PL emission spectrum of the donor (F_D), and can be calculated in units of M^{-1} cm^{-1} nm^4 using the equation:

$$J(\lambda) = \int_0^\infty \varepsilon_A(\lambda)\lambda^4 F_D(\lambda) d\lambda \quad (2)$$

where, $\varepsilon(\lambda)$ is the molar extinction coefficient of O-IDTT-IC(4FIC) at the wavelength λ which can be given by:

$$\varepsilon_A(\lambda) = \frac{\alpha(\lambda) M_\omega}{d} \quad (3)$$

in there, M_ω represents the molecular weight, d represents density of material (a usually value of d is 1.2kg/L), the $\alpha(\lambda)$ represents the films' absorption coefficients and can be calculated with the formula:

$$\alpha(\lambda) = \frac{OD \times ln(10)}{x} \quad (4)$$

in there, OD represents the absorbance of acceptors, the *x* represents films' thickness. The *ε(λ)* of both acceptors as shown in **Figure S3**. By these equations, the J(λ) between PTO2 and IDTT-IC or IDTT-4FIC are 4.47×10^{16} M^{-1} cm^{-1} nm^4 and 3.52×10^{16} M^{-1} cm^{-1} nm^4. Thus, the R_0 are 6.2 nm and 6.0 nm corresponding to PTO2/IDTT-IC and PTO2/IDTT-4FIC, respectively.

Table S1 | Neat film thickness of PTO2, IDTT-IC and IDTT-4FIC at different concentration. The spin coating speed of PTO2, IDTT-IC and IDTT-4FIC were 1500 rpm, 3000 rpm and 3000 rpm, respectively, as well as the film thickness is adjusted by changing the concentration.

Material	Solvent	Concentration (mg/ml)	Thickness[a] (nm)
PTO2	CB	8	35±2
IDTT-IC	DCM	2	15±1
IDTT-4FIC	DCM	2	16±2
IDTT-IC	DCM	8	61±4
IDTT-4FIC	DCM	8	63±6

[a] The average values obtained from 5 films.

4. Temperature-dependent PL spectra

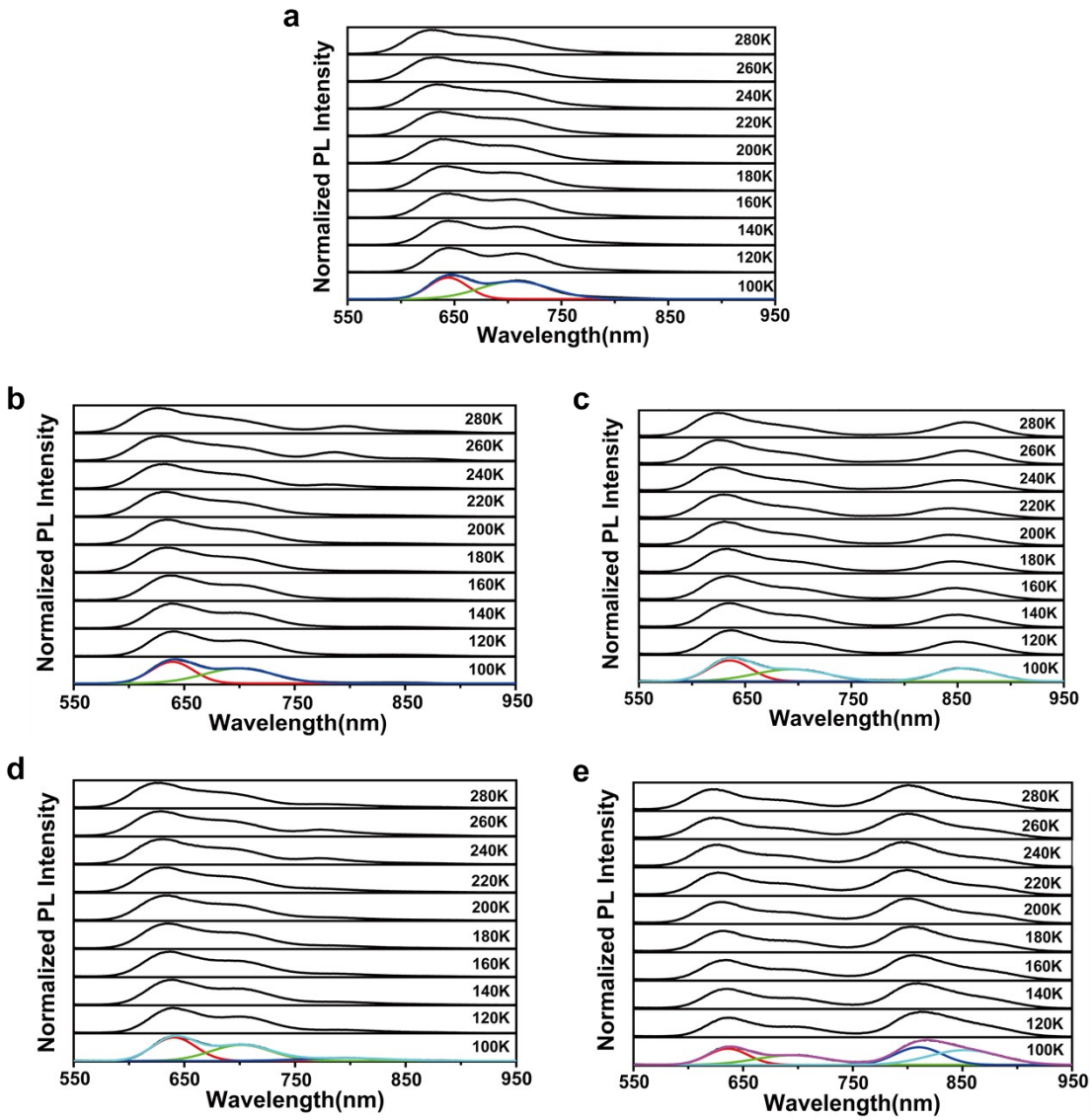

Fig. S4 | Temperature-dependent fluorescence spectra of the donor and donor/MoO_3/acceptor tandem films. a, pristine PTO2 **b,** PTO2/MoO_3/IDTT-IC (15 nm). **c,** PTO2/MoO_3/IDTT-IC (60 nm). **d,** PTO2/MoO_3/IDTT-4FIC (15 nm). **e,** PTO2/MoO_3/IDTT-4FIC (60 nm) as a function of substrate temperature. The

temperature ranged from 280 K to 100 K. Each PL spectrum was fitted with a Gaussian function to analyze the peaks.

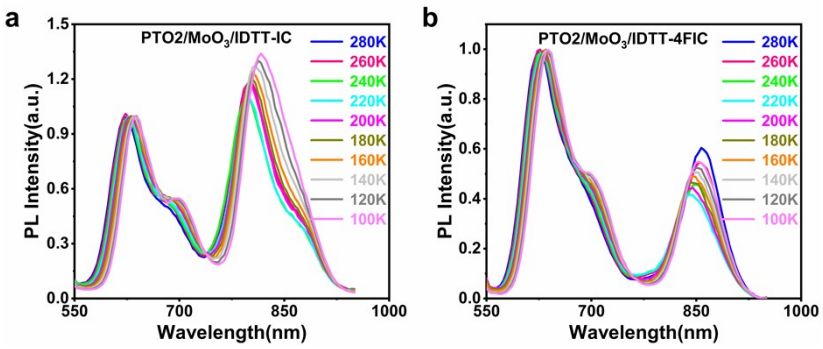

Fig. S5 | The Temperature-dependent PL spectra of PTO2/MoO_3/IDTT-IC (or IDTT-4FIC) which the thickness of IDTT-IC and IDTT-4FIC is 60 nm. The Temperature-dependent PL spectra of **a,** PTO2/IDTT-IC and **b,** PTO2/IDTT-4FIC which the PTO2 was normalized. The PL peak positions of donor and acceptors changed with temperature.

5. Devices structure

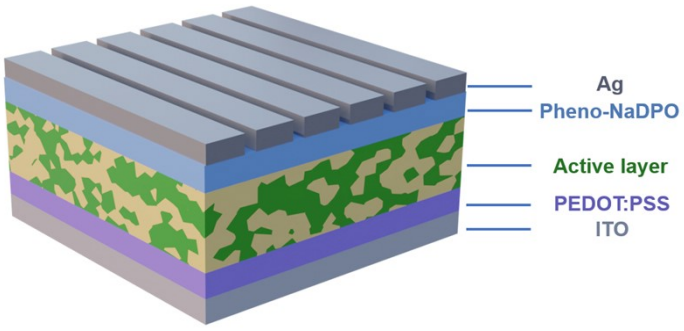

Fig. S6 | Device architecture diagrams BHJ devices based on PTO2:IDTT-IC or PTO2:IDTT-4FIC.

6. Performance of devices with PEDOT:PSS intercalation

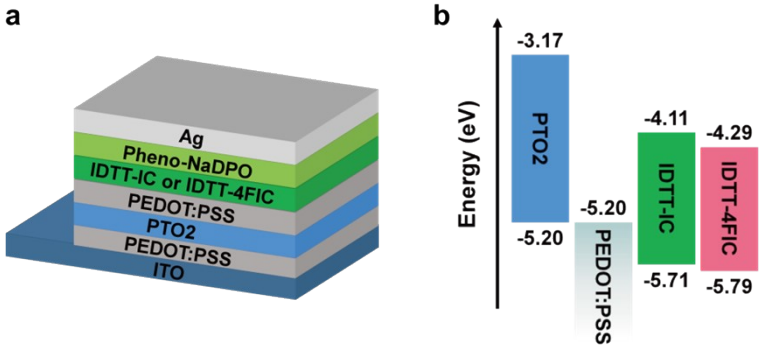

Fig. S7 | Schematic diagram and energy level of PTO2/PEDOT:PSS/IDTT-IC(or IDTT-4FIC). a, Schematic diagram of bilayer device and **b,** energy level of active layer. In there, PEDOT: PSS are insulating layers to isolate electron transfer, while FRET and HT are allowed. EQE spectra of PTO2/PEDOT:PSS/IDTT-IC.

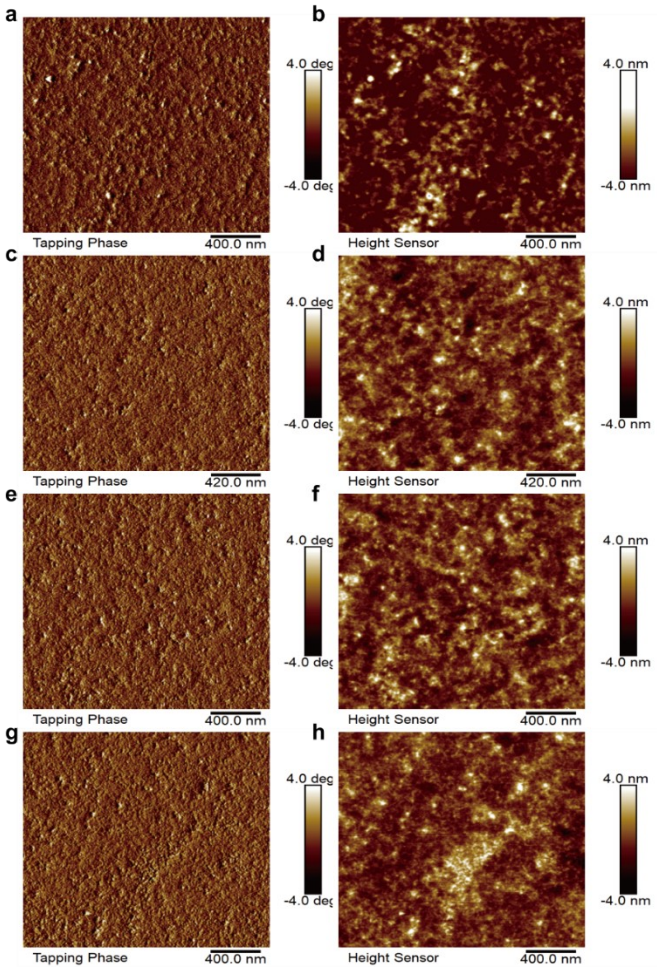

Fig. S8 │ AFM images of PEDOT:PSS. AFM images with spin coating speed of **(a, b,)** 1000rpm, **(c, d,)** 1333rpm, (**e, f,)** 2000rpm and (**g, h,)** 2666rpm, respectively.

Table S2 │ Photovoltaic parameters of the devices with PEDOT:PSS intercalation. The thickness of PTO2 and IDTT-IC (or IDTT-4FIC) are 35 nm and 60 nm, respectively.

Structure	PEDOT:PSS layer spin speed	J_{SC} (mA/cm^2)	V_{OV}(V)	FF	PCE_{ave}[a](%)
PTO2/PEDOT:PSS / IDTT-IC	1000	1.25±0.27	0.40±0.09	0.29±0.01	0.15±0.08
	1333	2.24±0.50	0.54±0.05	0.32±0.01	0.39±0.08
	2000	4.55±0.92	0.79±0.06	0.37±0.03	1.36±0.38
	2666	6.67±0.61	0.93±0.02	0.41±0.02	2.56±0.33
PTO2/PEDOT:PSS / IDTT-4FIC	1000	2.64±0.73	0.31±0.06	0.28±0.01	0.24±0.12
	1333	4.17±0.35	0.55±0.10	0.33±0.01	0.76±0.17
	2000	9.14±1.21	0.78±0.06	0.43±0.03	3.11±0.85
	2666	13.07±0.60	0.86±0.01	0.51±0.02	5.69±0.57

[a] The average values obtained from 20 devices for each condition.

Table S3 | Photovoltaic parameters of the devices covered by a short pass filter (<610nm).

Structure	PEDOT:PSS layer spin speed	J_{SC} (mA/cm^2)	V_{OV}(V)	FF	PCE_{ave}[a](%)
PTO2/PEDOT:PSS / IDTT-IC	1000	0.80±0.13	0.34±0.08	0.28±0.01	0.08±0.03
	1333	1.40±0.16	0.52±0.01	0.31±0.01	0.23±0.03
	2000	2.72±0.32	0.77±0.04	0.37±0.03	0.78±0.18
	2666	3.87±0.14	0.91±0.01	0.42±0.02	1.48±0.11
PTO2/PEDOT:PSS / IDTT-4FIC	1000	1.58±0.36	0.21±0.09	0.27±0.01	0.10±0.06
	1333	2.51±0.01	0.38±0.14	0.29±0.03	0.29±0.13
	2000	4.67±0.37	0.76±0.07	0.43±0.03	1.55±0.38
	2666	6.40±0.09	0.85±0.01	0.55±0.01	2.99±0.09

[a] The average values obtained from 20 devices for each condition.

Table S4 | Photovoltaic parameters of the devices covered by a long pass filter (>710 nm).

Structure	PEDOT:PSS layer spin speed	J_{SC} (mA/cm^2)	V_{OV}(V)	FF[a]	PCE_{ave}[b](%)
PTO2/PEDOT:PSS / IDTT-IC	1000	0.27±0.04	0.23±0.04	0.27±0.01	0.02±0.01
	1333	0.47±0.03	0.27±0.02	0.27±0.01	0.03±0.01
	2000	0.95±0.09	0.58±0.06	0.36±0.02	0.20±0.06
	2666	1.20±0.28	0.77±0.01	0.42±0.02	0.38±0.07
PTO2/PEDOT:PSS / IDTT-4FIC	1000	0.72±0.15	0.12±0.05	0.25±0.01	0.02±0.01
	1333	1.12±0.07	0.26±0.12	0.28±0.01	0.08±0.05
	2000	2.43±0.32	0.69±0.10	0.43±0.05	0.75±0.29
	2666	3.79±0.11	0.83±0.02	0.54±0.03	1.69±0.09

[a] FF represents the fill factor. [b] The average values obtained from 20 devices for each condition.

7. Photovoltaic performance of the BHJ OSCs

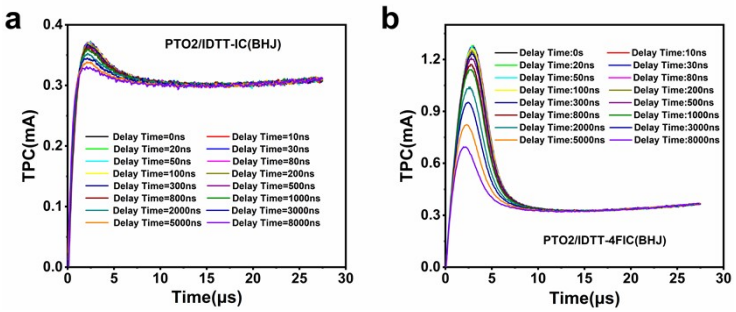

Fig. S9 | The photo-CELIV measurements of different structrues. TPC curves of **a,** PTO2/IDTT-IC, **b,** PTO2/IDTT-4FIC were obtained by photo-CELIV measurements.

8. References

(1) Y. Firdaus, L. P. Maffei, F. Cruciani, M. A. Müller, S. Liu, S. Lopatin, N. Wehbe, G. O. N. Ndjawa, A. Amassian, F. Laquai and P. M. Beaujuge. *Adv. Energy Mater.* 2017, **7**, 1700834.

(2) L. Benatto, C. A. M. Moraes, G. Candiotto, K. R. A. Sousa, J. P. A. Souza, L. S. Roman and M. Koehler. *J. Mater. Chem. A.* 2021, **9,** 27568–27585.

(3) T. Goh, J. S. Huang, B. Bartolome, M. Y. Sfeir, M. Vaisman, M. L. Leec and A. D. Taylor. *J. Mater. Chem. A*. 2015, **3,** 18611–18621.

(4) G. F. Burkhard, E. T. Hoke and M. D. McGehee. *Adv. Mater.* 2010, **22,** 3293–3297.